INTERNATIONAL JOURNAL OF ROBUST AND NONLINEAR CONTROL
Int. J. Robust Nonlinear Control 2015; **25**:1548–1568
Published online 11 March 2014 in Wiley Online Library (wileyonlinelibrary.com). DOI: 10.1002/rnc.3159

Nonlinear fractional-order power system stabilizer for multi-machine power systems based on sliding mode technique

Sajjad Shoja Majidabad*,†, Heydar Toosian Shandiz and Amin Hajizadeh

Department of Electrical and Robotic Engineering, Shahrood University of Technology, Shahrood, Iran

SUMMARY

This paper presents two novel nonlinear fractional-order sliding mode controllers for power angle response improvement of multi-machine power systems. First, a nonlinear block control is used to handle nonlinearities of the interconnected power system. In the second step, a decentralized fractional-order sliding mode controller with a nonlinear sliding manifold is designed. Practical stability is achieved under the assumption that the upper bound of the fractional derivative of perturbations and interactions are known. However, when an unknown transient perturbation occurs in the system, it makes the evaluation of perturbation and interconnection upper bound troublesome. In the next step, an adaptive-fuzzy approximator is applied to fix the mentioned problem. The fuzzy approximator uses adjacent generators relative speed as own inputs, which is known as semi-decentralized control strategy. For both cases, the stability of the closed-loop system is analyzed by the fractional-order stability theorems. Simulation results for a three-machine power system with two types of faults are illustrated to show the performance of the proposed robust controllers versus the conventional sliding mode. Additionally, the fractional parameter effects on the system transient response and the excitation voltage amplitude and chattering are demonstrated in the absence of the fuzzy approximator. Finally, the suggested controller is combined with a simple voltage regulator in order to keep the system synchronism and restrain the terminal voltage variations at the same time. Copyright © 2014 John Wiley & Sons, Ltd.

Received 3 August 2013; Revised 16 January 2014; Accepted 23 January 2014

KEY WORDS: fractional calculus; sliding mode control; decentralized and semi-decentralized control; nonlinear block control; multi-machine power system; power angle stability; fuzzy approximation

1. INTRODUCTION

Large-scale power systems are incessantly getting larger in size and complexity with increasing interconnections. They consist of several synchronous generators having the different inertia constants, which are weakly connected through large transmission lines. One of the most crucial operation demands of power systems is maintaining the system stability. Conventional decentralized linear power system stabilizers (PSS) were well applied because of their simplicity in design and implementation. Such linear PSS is limited because it provides stability in a small region and only deals with small disturbances around an operating point. Then, when some large perturbations transpire, the synchronism among the power system generators can be lost [1, 2].

In last two decades, researchers are focused on nonlinear control techniques to design robust and reliable PSSs for power systems. Some works deal with the decentralized control of multi-machine power system based on direct feedback linearization (DFL) technique in [3, 4], DFL with backstepping [5] and adaptive backstepping techniques [6]. Recently, the sliding mode control (SMC) has been applied for power systems, because this method is well known for its high precision and

*Correspondence to: Sajjad Shoja Majidabad, Department of Electrical and Robotic Engineering, Shahrood University of Technology, Shahrood, Iran.
†E-mail: shoja.sajjad@gmail.com

robustness against model uncertainties and perturbations [7]. The SMC with nonlinear block control (NBC) technique is implemented to control a single-machine connected to an infinite bus in [8, 9], and a multi-machine power system [10, 11]. This method also is designed based on output information [12], and in the higher-order form [13, 14]. Additionally, the SMC is applied to control a complete model power system with match and mismatch uncertainties [15], and a simplified second-order model in [16]. All of the mentioned papers have been developed based on integer-order calculus.

Fractional calculus is an old mathematical with a generalization of ordinary differentiation-integration to an arbitrary order. Nearly 300 years, this branch of mathematics was viewed as an only theoretical topic with no practical applications [17]. But in last three decades, it has been used in different fields of engineering and physics such as: electrical circuit [18], rotor-bearing system [19], finance system [20], biological system [21], thermoelectric system [22], reaction–diffusion system [23], and finally designing fractional-order controllers on fractional and integer-order systems is a dominant part of these applications.

Recently, designing the fractional-order controllers on fractional-order systems has been developed. For instant, there are some valuable literatures especially in sliding mode control of fractional-order chaotic systems [24–28]. But in reality, most of physical systems have inherently integer-order dynamics. Therefore, enlarging the application of fractional-order controllers on integer-order systems seems more practical in spite of its challenges. Moreover, fractional-order controllers give us some extra parameters for tuning, which can lead to a better closed-loop performance.

The main idea of fractional-order controller application on integer-order systems is debated in [29]. In this paper, based on an example, the authors proofed that better tracking is achievable for non-integer orders. This is a remarkable idea, but it is not extendable for all integer-order systems, and optimal parameters may lie on the integer-order values ([17], section 9.2.4). In this situation, fractional-order controllers are not able to reach a better performance in comparison with the integer-order ones. Therefore, in addition to the integer-order system characteristics, choosing a suitable fractional-order controller is necessary in order to obtain a superior behavior.

As mentioned earlier, fractional-order controllers provide extra parameters for tuning. Hence, using this idea in modern nonlinear control techniques like SMC can be useful. Recently, fractional-order sliding mode controller (FSMC) has been used for integer-order systems such as robot manipulators [30], permanent magnet synchronous machines [31, 32], antilock braking systems [33], and induction motor [34]. Additionally, FSMC with nonlinear sliding surface has been applied in [35]. Some of these works are common in the following cases: (1) Using a linear sliding manifold: the main disadvantage of linear sliding manifold is that the system states cannot reach the equilibrium point in a finite time. By defining special nonlinear types of sliding surface, faster convergence is accessible [35]. (2) Designing some controllers for small-scale systems: while multi-machine power system is a large-scale system composed of multiple synchronous generators. (3) Applying integer-order stability theorems: a closed-loop system is fractional-order if controller or system or both of them be fractional-order. Therefore, using fractional-order stability theorems will be useful for stability analyzing of the fractional-order closed-loop systems.

Inspired by the aforementioned discussions, combination of the NBC technique [36, 37] with nonlinear fractional-order sliding mode controllers (NFSMC) is used to design fast and robust PSSs in this paper. Generally, this paper presents the following main contributions: (1) A new nonlinear fractional-order sliding surface is proposed to reach a faster transient response. (2) Two decentralized and semi-decentralized fractional-order controllers are developed to halter the multi-machine power system. (3) Stability of the closed–loop system is analyzed based on fractional-order stability theorems.

The remainder of this paper is organized as follows: in Section 2, some preliminaries and properties of fractional-order calculus are introduced. A third-order multi-machine power system nonlinear model is presented in Section 3. In Section 4, the NBC technique is applied to provide a proper model. A decentralized NFSMC PSS is developed in Section 5. Section 6 describes a semi-decentralized NFSMC PSS, which covers the perturbation and interconnection

DOI: 10.1002/rnc

problem. In Section 7, simulation results are illustrated and finally, conclusions are presented in Section 8.

2. PRELIMINARIES

In this section, we state some definitions, properties, and theorems, which will be used later.

Definition 1 ([38]*)*
The function $f(t) : \mathbb{R} \to \mathbb{R}$ is continuously differentiable if $f(t)$ be differentiable and $\dot{f}(t)$ be continuous.

From this definition, $f(t) \in C^0, C^1$ and C^∞ are the classes of continuous, continuously differentiable and smooth functions, respectively.

Definition 2 ([39]*)*
The α-th order Riemann–Liouville fractional integration of function $f(t)$ with respect to t is given by

$$I^{\alpha}_{0,t} f(t) = D^{-\alpha}_{0,t} f(t) = \frac{1}{\Gamma(\alpha)} \int_0^t \frac{f(\tau)}{(t-\tau)^{1-\alpha}} d\tau \tag{1}$$

where $\Gamma(\alpha)$ is the Gamma function.

Definition 3 ([39]*)*
The Grunwald–Letnikov (GL) fractional derivative of function $f(t)$ with fractional-order α is given by

$${}_{GL}D^{\alpha}_{0,t} f(t) = \sum\nolimits_{k=0}^{m-1} \frac{f^{(k)}(0) t^{-\alpha+k}}{\Gamma(-\alpha+k+1)} + \frac{1}{\Gamma(m-\alpha)} \int_0^t \frac{f^{(m)}(\tau)}{(t-\tau)^{1-m+\alpha}} d\tau \tag{2}$$

where $f(t) \in C^m[0,t]$ and $m-1 \leqslant \alpha < m, m \in \mathbb{N}$.

Definition 4 ([39]*)*
The α-th order Caputo fractional derivative of continuous ($f(t) \in C^m[0,t]$) function $f(t)$ is defined as follows:

$${}_{C}D^{\alpha}_{0,t} f(t) = D^{-(m-\alpha)}_{0,t} D^m f(t) = \frac{1}{\Gamma(m-\alpha)} \int_0^t \frac{f^{(m)}(\tau)}{(t-\tau)^{1-m+\alpha}} d\tau \tag{3}$$

where $m-1 < \alpha < m, m \in \mathbb{N}$.

Definition 5 ([39]*)*
The α-th order Riemann–Liouville (RL) fractional derivative of function $f(t)$ is given as follows:

$${}_{RL}D^{\alpha}_{0,t} f(t) = D^m D^{-(m-\alpha)}_{0,t} f(t) = \frac{1}{\Gamma(m-\alpha)} \frac{d^m}{dt^m} \int_0^t \frac{f(\tau)}{(t-\tau)^{1-m+\alpha}} d\tau \tag{4}$$

where $m-1 \leqslant \alpha < m, m \in \mathbb{N}$.

Property 1 ([39]*)*
If $f(t) \in C^0[0,T]$ for $T > 0$ and $\alpha > 0$, then

$$D^{-\alpha}_{0,t} f(t)|_{t=0} = 0 \tag{5}$$

Property 2 ([39]*)*
If $f(t) \in C^m[0,\infty)$, $m-1 < \alpha < m$ and $m \in \mathbb{N}$, then

(a) ${}_{C}D^{\alpha}_{0,t} f(t) = {}_{RL}D^{\alpha}_{0,t} \left(f(t) - \sum_{k=0}^{m-1} \frac{t^k}{k!} f^{(k)}(0) \right)$.

(b) ${}_{RL}D^{\alpha}_{0,t} D^{-\alpha}_{0,t} f(t) = f(t)$.

(c) ${}_{C}D^{\alpha}_{0,t} D^{-\alpha}_{0,t} f(t) = f(t)$ holds for $m = 1$.

DOI: 10.1002/rnc

Part (c) proof: Using parts (a), (b), and Property 1, leads to

$$ {}_C D^{\alpha}_{0,t}\left(D^{-\alpha}_{0,t} f(t)\right) = {}_{RL} D^{\alpha}_{0,t}\left(D^{-\alpha}_{0,t} f(t) - D^{-\alpha}_{0,t} f(t)|_{t=0}\right) = {}_{RL} D^{\alpha}_{0,t}\left(D^{-\alpha}_{0,t} f(t) - 0\right) = f(t) \quad (6) $$

Property 3 (sequential property [39]*)*
If $f(t) \in C^1[0,T]$ for some $T > 0, \alpha_i \in (0,1)(i = 1,2)$ and $\alpha_1 + \alpha_2 \in (0,1]$, then

$$ {}_C D^{\alpha_1}_{0,t} {}_C D^{\alpha_2}_{0,t} f(t) = {}_C D^{\alpha_2}_{0,t} {}_C D^{\alpha_1}_{0,t} f(t) = {}_C D^{\alpha_1+\alpha_2}_{0,t} f(t) \quad (7) $$

Note that the continuously differentiability condition restricts the sequential property. To prove this idea, two examples are illustrated in Table I. The first function does not satisfy (7) as a result of discontinuity at $t = 0$.

Generally, for a finite number of discontinuous points of $\dot{f}(t)$, the function $f(t)$ still can be assumed continuously differentiability.

Remark 1
Let us consider the sliding surface $s(t) = f(t), \alpha_1 = \alpha$ and $\alpha_2 = 1-\alpha$, then (7) will be as follows:

$$ \dot{s}(t) = {}_C D^{\alpha}_{0,t} {}_C D^{1-\alpha}_{0,t} s(t) = {}_C D^{1-\alpha}_{0,t} {}_C D^{\alpha}_{0,t} s(t) \quad (8) $$

from mathematical point of view and according to Property 3, equation (8) holds for continuous $s(t)$ and $\dot{s}(t)$, whereas discontinuous function $sgn(s(t))$, non-smooth desired values, and sudden changes in disturbances may cause discontinuous $\dot{s}(t)$, which degrades C^1 condition. Using fuzzy approximations, smooth functions $(\tanh(s(t)), sat(s(t)), D^{-\alpha}_{0,t} s(t))$ instead of $sgn(s(t))$ and smooth desired values are approximate practical remedies for the mentioned problem.

Definition 6 ([40, 41]*)*
The solution of the system ${}_C D^{\alpha}_{0,t} x(t) = f(t, x(t))$ is said to be Mittag–Leffler stable if

$$ \|x(t)\| \leqslant \{m[x(0)] E_{\alpha}(-\lambda t^{\alpha})\}^b \quad (9) $$

where $\alpha \in (0,1), \lambda > 0, b > 0, E_{\alpha}(t)$ is the Mittag–Leffler function, $m(0) = 0$ and $m(x) \geqslant 0$ is locally Lipschitz.

Remark 2
It is evident that the Mittag–Leffler stability implies the asymptotic stability.

Theorem 1 ([40]*)*
Let $x = 0$ be an equilibrium point for the non-autonomous fractional-order system

$$ {}_C D^{\alpha}_{0,t} x(t) = f(t, x(t)) \quad (10) $$

Table I. Two examples of sequential property.

Function	$f(t)$	$\dot{f}(t)$	Property 3 ($\alpha_1 = 1/3$, $\alpha_2 = 1/2$)
		Discontinuous	
$f_1(t) = t^{0.5}$	Continuous	$\dot{f}_1(t) = 0.5t^{-0.5}$	${}_C D^{\alpha_1+\alpha_2}_{0,t} f_1(t) = {}_C D^{\alpha_2}_{0,t} {}_C D^{\alpha_1}_{0,t} f_1(t) = \frac{\Gamma(3/2)}{\Gamma(2/3)} t^{-1/3}$
		$\dot{f}_1(0^+) \to +\infty$	${}_C D^{\alpha_1}_{0,t} {}_C D^{\alpha_2}_{0,t} f_2(t) = 0$
		Continuous	
$f_2(t) = t^{1.5}$	Continuous	$\dot{f}_2(t) = 1.5t^{0.5}$	${}_C D^{\alpha_1+\alpha_2}_{0,t} f_2(t) = {}_C D^{\alpha_1}_{0,t} {}_C D^{\alpha_2}_{0,t} f_2(t) = {}_C D^{\alpha_2}_{0,t}$
		$\dot{f}_2(0) = 0$	${}_C D^{\alpha_1}_{0,t} f_2(t) = \frac{\Gamma(5/2)}{\Gamma(5/3)} t^{2/3}$

DOI: 10.1002/rnc

where $f(t, x(t))$ satisfies the Lipschitz condition with Lipschitz constant $l > 0$ and $\alpha \in (0, 1)$. Assume that there exists a Lyapunov function $V(t, x(t))$ satisfying

$$\alpha_1 \|x\|^a \leqslant V(t, x(t)) \leqslant \alpha_2 \|x\| \tag{11}$$

$$\frac{d}{dt} V(t, x(t)) \leqslant -\alpha_3 \|x\| \tag{12}$$

where $\alpha_1, \alpha_2, \alpha_3$ and a are positive constants. Then, the equilibrium point of the system (10) is Mittag–Leffler stable.

Theorem 2 ([40, 41]*)*
Let $x = 0$ be an equilibrium point for the non-autonomous fractional-order system (10). Assume that there exists a Lyapunov function $V(t, x(t))$ and class-K functions $\alpha_i (i = 1, 2, 3)$ satisfying

$$\alpha_1(\|x\|) \leqslant V(t, x(t)) \leqslant \alpha_2(\|x\|) \tag{13}$$

$${}_C D^{\beta}_{0,t} V(t, x(t)) \leqslant -\alpha_3(\|x\|) \tag{14}$$

where $\beta \in (0, 1)$. Then, the system (10) is asymptotically stable.

Corollary 1 ([42]*)*
Form Theorem 2, if ${}_C D^{\beta}_{0,t} V(t, x(t)) \leqslant 0$, then the system (10) is locally stable.

Proof
From ${}_C D^{\beta}_{0,t} V(t, x(t)) \leqslant 0$, we can get $V(t, x(t)) \leqslant V(0, x(0))$. Taking into account (13), results $\|x\| \leqslant \alpha_1^{-1}(V(t, x(t))) \leqslant \alpha_1^{-1}(V(0, x(0)))$. Therefore, the equilibrium point $x = 0$ is stable. □

3. POWER SYSTEM DYNAMICAL MODEL

In this section, a multi-machine power system consisting of n synchronous generators is considered. A third-order dynamic model of the i-th generator with excitation control can be described as follows [4–6]:

Generator mechanical equations:

$$\dot{\delta}_i(t) = \Delta\omega_i(t) \tag{15}$$

$$\Delta\dot{\omega}_i(t) = -\frac{D_i}{2H_i}\Delta\omega_i(t) - \frac{\omega_0}{2H_i}\left(P_{ei}(t) - P_{mi0}\right) \tag{16}$$

where $\delta_i(t)$ is the power or load angle of the generator (rad); $\Delta\omega_i(t)$ is the relative speed of generator (rad/sec); P_{mi0} is the mechanical input power $(p.u.)$; $P_{ei}(t)$ is the active electrical power delivered by the generator $(p.u.)$; ω_0 is the synchronous speed (rad/sec); D_i is per unit damping constant and H_i is the inertia constant (sec).

Generator electrical dynamics:

$$\dot{E}^{'}_{qi}(t) = \frac{1}{T^{'}_{doi}}\left(E_{fi}(t) - E_{qi}(t)\right) \tag{17}$$

where $E^{'}_{qi}(t)$ is the transient Electromotive Force (EMF) in the quadrature axis of the generator $(p.u.)$; $E_{qi}(t)$ is the EMF in the quadrature axis $(p.u.)$; $E_{fi}(t)$ is the equivalent EMF in the excitation coil $(p.u.)$ and $T^{'}_{doi}$ is the direct axis transient short circuit time constant (sec).

Electrical equations:

$$E_{qi}(t) = E^{'}_{qi}(t) - \left(x_{di} - x^{'}_{di}\right) I_{di}(t) \tag{18}$$

DOI: 10.1002/rnc

$$P_{ei}(t) = \sum_{j=1}^{n} E'_{qi}(t)E'_{qj}(t)B_{ij}\sin\left(\delta_i(t) - \delta_j(t)\right) = E'_{qi}(t)I_{qi}(t) \tag{19}$$

$$Q_{ei}(t) = -\sum_{j=1}^{n} E'_{qi}(t)E'_{qj}(t)B_{ij}\cos\left(\delta_i(t) - \delta_j(t)\right) = -E'_{qi}(t)I_{di}(t) \tag{20}$$

$$I_{di}(t) = \sum_{j=1}^{n} E'_{qj}(t)B_{ij}\cos\left(\delta_i(t) - \delta_j(t)\right) \tag{21}$$

$$I_{qi}(t) = \sum_{j=1}^{n} E'_{qj}(t)B_{ij}\sin\left(\delta_i(t) - \delta_j(t)\right) \tag{22}$$

$$E_{fi}(t) = k_{ci}u_{fi}(t) \tag{23}$$

$$E_{qi}(t) = x_{adi}I_{fi}(t) \tag{24}$$

$$V_{ti}(t) = \sqrt{\left(E'_{qi}(t) + x'_{di}I_{di}(t)\right)^2 + \left(x'_{di}I_{qi}(t)\right)^2} \tag{25}$$

where $Q_{ei}(t)$ is the reactive power $(p.u.)$; $I_{di}(t)$ is the direct axis current $(p.u.)$; $I_{qi}(t)$ is the quadrature axis current $(p.u.)$; B_{ij} is the i-th row and j-th column element of nodal susceptance matrix at the internal nodes after eliminating all physical buses $(p.u.)$; $u_{fi}(t)$ is the input of the Silicon Controlled Rectifier (SCR) amplifier $(p.u.)$; k_{ci} is the gain of the excitation amplifier $(p.u.)$; $I_{fi}(t)$ is the excitation current $(p.u.)$; x_{adi} is the mutual reactance between the excitation coil and the stator coil of the i-th generator $(p.u.)$; x_{di} is the direct axis reactance $(p.u.)$; x'_{di} is the direct axis transient reactance $(p.u.)$; $V_{ti}(t)$ is the terminal voltage of the i-th generator $(p.u.)$.

Since $\dot{E}'_{qi}(t)$ is not physically measurable, then it can be removed by differentiating (19) and substituting (17) in it. Therefore, the i-th generator model with new set of variables $(\delta_i, \Delta\omega_i, \Delta P_{ei})$, will be in the following form:

$$\begin{cases} \dot{\delta}_i(t) = \Delta\omega_i(t) \\ \Delta\dot{\omega}_i(t) = -\frac{D_i}{2H_i}\Delta\omega_i(t) - \frac{\omega_0}{2H_i}\left(P_{ei}(t) - P_{mi0}\right) \\ \Delta\dot{P}_{ei}(t) = -\frac{1}{T'_{d0i}}\left(\Delta P_{ei}(t) + P_{mi0} - (x_{di} - x'_{di})I_{qi}(t)I_{di}(t)\right) - Q_{ei}(t)\Delta\omega_i(t) \\ \qquad\qquad + \frac{1}{T'_{d0i}}k_{ci}I_{qi}(t)u_{fi}(t) + \gamma_i(\delta,\omega) \end{cases} \tag{26}$$

that

$$\Delta P_{ei}(t) = P_{ei}(t) - P_{mi0} \tag{27}$$

$$\gamma_i(\delta,\omega) = \sum_{j=1}^{n} E'_{qi}(t)\dot{E}'_{qj}(t)B_{ij}\sin\left(\delta_i(t) - \delta_j(t)\right) - \sum_{j=1}^{n} E'_{qi}(t)E'_{qj}(t)B_{ij}\cos\left(\delta_i(t) - \delta_j(t)\right) \tag{28}$$

where $\gamma_i(\delta,\omega)$ is the interconnection term among the i-th generator with the others.

Assumption 1

The mechanical input power P_{mi0} is assumed to be a constant because it is associated with very slow time constants.

Remark 3

From Remark 3.4. in [3], because the active $P_{ei}(t)$ and reactive $Q_{ei}(t)$ powers of each generator and power flow through each transmission line are bounded, and the excitation voltage $E_{fi}(t)$ may increase by up to five times of the $E'_{qi}(t)$, then we have

$$|\gamma_i(\delta,\omega)| \leq \sum_{j=1}^{n}\left(\gamma_{i1j}\left|\sin(\delta_j)\right| + \gamma_{i2}\left|\Delta\omega_j\right|\right) \leq \sum_{j=1}^{n}\left(\gamma_{i1j} + \gamma_{i2}\left|\Delta\omega_j\right|\right) \tag{29}$$

DOI: 10.1002/rnc

where

$$\gamma_{i1j} = \begin{cases} \sum_{j=1,j\neq i}^{n} 4p_{1ij}\frac{|P_{ei}|_{max}}{|T'_{doj}|_{min}} & j = i \\ 4p_{1ij}\frac{|P_{ei}|_{max}}{|T'_{doj}|_{min}} & j \neq i \end{cases}, \quad \gamma_{i2} = p_{2ij}\,|Q_{ei}|_{max} \tag{30}$$

where p_{1ij} and p_{2ij} values are 0 or 1 (if they are 0, it means that there is no connection between j-th and i-th generators).

4. NONLINEAR BLOCK CONTROL TECHNIQUE

From [36, 37], it can be seen that the i-th subsystem (26) has NBC-form composed of three blocks. Therefore, the NBC technique can be applied before designing the SMC. The equation (26) non-companion form is the main reason of applying the NBC before SMC.

Because the control goal is the power angle performance enhancement for the generators in the presence of interconnections and perturbations, then output error can be defined as follows:

$$z_{1i}(t) = \delta_i(t) - \delta_{di} \tag{31}$$

where δ_{di} is a known constant reference signal. Then, using (26) and (31), we obtain

$$\dot{z}_{1i}(t) = \Delta\omega_i(t) \tag{32}$$

To stabilize (32) dynamics, the virtual control input is chosen as

$$\Delta\omega_i(t) = -k_{1i}z_{1i}(t) + z_{2i}(t), \quad k_{1i} > 0 \tag{33}$$

Hence, z_{1i} closed-loop dynamic will be as

$$\dot{z}_{1i}(t) = -k_{1i}z_{1i}(t) + z_{2i}(t) \tag{34}$$

In the next step, from (32) and (34), the new variable z_{2i} can be obtained as

$$z_{2i}(t) = \Delta\omega_i(t) + k_{1i}z_{1i}(t) \tag{35}$$

By differentiating (35), and using (26) and (34), results in

$$\dot{z}_{2i}(t) = -\frac{\omega_0}{2H_i}\Delta P_{ei}(t) + \left(\frac{D_i k_{1i}}{2H_i} - k_{1i}^2\right)z_{1i}(t) + \left(k_{1i} - \frac{D_i}{2H_i}\right)z_{2i}(t) \tag{36}$$

Considering ΔP_{ei} as the virtual control input in (36), we choose

$$\Delta P_{ei}(t) = \frac{2H_i}{\omega_0}\left(\left(\frac{D_i k_{1i}}{2H_i} - k_{1i}^2\right)z_{1i}(t) + \left(k_{1i} - \frac{D_i}{2H_i}\right)z_{2i}(t) + k_{2i}z_{2i}(t) - z_{3i}(t)\right), \quad k_{2i} > 0 \tag{37}$$

By substituting (37) in (36), the second block closed-loop dynamic will be as

$$\dot{z}_{2i}(t) = -k_{2i}z_{2i}(t) + z_{3i}(t) \tag{38}$$

At the third step, the new variable z_{3i} can be obtained from (36) and (38) as follows:

$$z_{3i}(t) = -\frac{\omega_0}{2H_i}\Delta P_{ei}(t) + \left(\frac{D_i k_{1i}}{2H_i} - k_{1i}^2\right)z_{1i}(t) + \left(k_{1i} + k_{2i} - \frac{D_i}{2H_i}\right)z_{2i}(t) \tag{39}$$

By differentiating (39) and using (26), (34), and (38), the third block dynamic will be as follows:

DOI: 10.1002/rnc

$$\dot{z}_{3i}(t) = g_i\left(z_{1i}, z_{2i}, z_{3i}\right) + \frac{\omega_0}{2H_i T'_{doi}}\Big(\Delta P_{ei}(t) + P_{mi0} - (x_{di} - x'_{di}) I_{qi}(t) I_{di}(t) + T'_{doi} Q_{ei}(t)\Delta\omega_i(t)\Big) - \frac{\omega_0}{2H_i T'_{doi}} k_{ci} I_{qi}(t) u_{fi}(t) - \frac{\omega_0}{2H_i}\gamma_i(\delta,\omega) \tag{40}$$

where

$$g_i(z_{1i}, z_{2i}, z_{3i}) = \left(k_{1i}^3 - \frac{D_i k_{1i}^2}{2H_i}\right) z_{1i}(t) + \left(\frac{D_i k_{1i}}{2H_i} - k_{1i}^2 - k_{2i}\left(k_{1i} + k_{2i} - \frac{D_i}{2H_i}\right)\right) \times z_{2i}(t) + \left(k_{1i} + k_{2i} - \frac{D_i}{2H_i}\right) z_{3i}(t) \tag{41}$$

Finally, the i-th subsystem (26) can be rewritten by the following transformed form:

$$\begin{cases} \dot{z}_{1i}(t) = -k_{1i} z_{1i}(t) + z_{2i}(t) \\ \dot{z}_{2i}(t) = -k_{2i} z_{2i}(t) + z_{3i}(t) \\ \dot{z}_{3i}(t) = g_i\left(z_{1i}, z_{2i}, z_{3i}\right) + \frac{\omega_0}{2H_i T'_{doi}}\left(\Delta P_{ei}(t) + P_{mi0} - \left(x_{di} - x'_{di}\right) I_{qi}(t) I_{di}(t) + T'_{doi} Q_{ei}(t)\Delta\omega_i(t)\right) \\ \qquad -\frac{\omega_0}{2H_i T'_{doi}} k_{ci} I_{qi}(t) u_{fi}(t) - \frac{\omega_0}{2H_i}\gamma_i(\delta,\omega) \end{cases} \tag{42}$$

where k_{1i} and k_{2i} are known as control gains.

Assumption 2
To avoid $I_{qi}(t) = 0$, assume that the generators are operating in the normal working region ($0 < \delta_i < \pi$ and $\delta_i \neq \delta_j$).

5. DECENTRALIZED NFSMC DESIGN

In this section, a decentralized nonlinear fractional-order sliding-mode PSS for the multi-machine power system (42) is developed. For this purpose, a nonlinear fractional-order sliding surface based on the fractional-order reaching law is proposed. The suggested controller is designed based on the Caputo derivative.

Let the nonlinear fractional-order sliding surface to be defined as follows:

$$s_i(t) = {}_C D^{1-\alpha} z_{3i}(t) + \lambda_i D^{-\alpha} z_{3i}^{p_i/q_i}(t) \tag{43}$$

where $0 < \alpha < 1, \lambda_i > 0$, p_i and q_i are odd integers satisfying $q_i > p_i > 0$. Taking ${}_C D^{\alpha}$ derivative from both sides of (43), leads to

$${}_C D^{\alpha} s_i(t) = {}_C D^{\alpha}\, {}_C D^{1-\alpha} z_{3i}(t) + \lambda_i\, {}_C D^{\alpha} D^{-\alpha} z_{3i}^{p_i/q_i}(t) \tag{44}$$

From Properties 2.c and 3, we get

$${}_C D^{\alpha} s_i(t) = \dot{z}_{3i}(t) + \lambda_i z_{3i}^{p_i/q_i}(t) \tag{45}$$

Substituting (42) into (45), results in

$${}_C D^{\alpha} s_i(t) = g_i\left(z_{1i}, z_{2i}, z_{3i}\right) + \frac{\omega_0}{2H_i T'_{doi}}\Big(\Delta P_{ei}(t) + P_{mi0} - (x_{di} - x'_{di}) I_{qi}(t) I_{di}(t) + T'_{doi} Q_{ei}(t)\Delta\omega_i(t)\Big) + \lambda_i z_{3i}^{p_i/q_i}(t) - \frac{\omega_0}{2H_i T'_{doi}} k_{ci} I_{qi}(t) u_{fi}(t) - \frac{\omega_0}{2H_i}\gamma_i(\delta,\omega) \tag{46}$$

DOI: 10.1002/rnc

Theorem 3
Consider the system (42) with the nonlinear sliding manifold (43) and assumption 1. The control law,

$$u_{fi}(t) = \frac{2H_i T'_{doi}}{\omega_0 k_{ci} I_{qi}(t)} \Bigg(g_i(z_{1i}, z_{2i}, z_{3i}) + \frac{\omega_0}{2H_i T'_{doi}} \Big(\Delta P_{ei}(t) + P_{mi0} - \Big(x_{di} - x'_{di} \Big) I_{qi}(t) I_{di}(t) \Big) + T'_{doi} Q_{ei}(t) \Delta\omega_i(t) + \lambda_i z_{3i}^{p_i/q_i}(t) + D^{-(1-\alpha)} \left(\eta_i s_i(t) + K_{sw-i} \tanh\left(s_i(t)/\rho_i\right) \right) \Bigg), \quad 0 < \rho_i < 1 \tag{47}$$

guarantees the closed-loop system asymptotical stability, if the switching gain K_{sw-i} be selected as

$$K_{sw-i} \geq \frac{\omega_0}{2H_i} \left| {}_C D^{1-\alpha} \gamma_i(\delta, \omega) \right| \tag{48}$$

then the transformed variables (z_{1i}, z_{2i}, z_{3i}) will converge to zero.

Proof
Consider the global continuously differentiable (except at $s_i(t) = 0$) Lyapunov candidate to be as follows:

$$V(t, s(t)) = \|s(t)\|_1 = \sum\nolimits_{i=1}^{n} V_i(t, s_i(t)) = \sum\nolimits_{i=1}^{n} |s_i(t)| \tag{49}$$

where $s = [s_1, s_2, \ldots, s_n]^T$ is the sliding surface vector of n generators and $V_i(t, s_i(t))$ is the Lyapunov function for each generator. By differentiating $V(t, s(t))$ with respect to time

$$\dot{V}(t, s(t)) = \sum\nolimits_{i=1}^{n} sgn(s_i(t)) \dot{s}_i(t) \tag{50}$$

Using Property 3, the following equation fractionalizes the integer-order derivative into a fractional type.

$$\dot{s}_i(t) = {}_C D^{1-\alpha} {}_C D^{\alpha} s_i(t) \tag{51}$$

Inserting (51) into (50), results in

$$\dot{V}(t, s(t)) = \sum\nolimits_{i=1}^{n} sgn(s_i(t)) \dot{s}_i(t) = \sum\nolimits_{i=1}^{n} sgn(s_i(t)) \left({}_C D^{1-\alpha} {}_C D^{\alpha} s_i(t) \right) \tag{52}$$

Using the sliding surface dynamics (45), one can obtain

$$\dot{V}(t, s(t)) = \sum\nolimits_{i=1}^{n} sgn(s_i(t)) {}_C D^{1-\alpha} \Bigg(g_i\left(z_{1i}, z_{2i}, z_{3i}\right) + \frac{\omega_0}{2H_i T'_{doi}} \left(\Delta P_{ei}(t) + P_{mi0} - \Big(x_{di} - x'_{di} \Big) I_{qi}(t) I_{di}(t) + T'_{doi} Q_{ei}(t) \Delta\omega_i(t) \right) + \lambda_i z_{3i}^{p_i/q_i}(t) - \frac{\omega_0}{2H_i T'_{doi}} k_{ci} I_{qi}(t) u_{fi}(t) - \frac{\omega_0}{2H_i} \gamma_i(\delta, \omega) \Bigg) \tag{53}$$

Substituting control signal (47) in (53), we get

$$\dot{V}(t, s(t)) = \sum\nolimits_{i=1}^{n} sgn(s_i(t)) {}_C D^{1-\alpha} \left(-D^{-(1-\alpha)} (\eta_i s_i(t) + K_{sw-i} \tanh\left(s_i(t)/\rho_i\right)) - \frac{\omega_0}{2H_i} \gamma_i(\delta, \omega) \right) \tag{54}$$

Because $\eta_i s_i(t) + K_{sw-i} \tanh\left(s_i(t)/\rho_i\right)$ is a continuously differentiable function, then from Property 2.c, we get

DOI: 10.1002/rnc

$$\dot{V}(t,s(t)) = -\sum_{i=1}^{n}\left(\eta_i\,|s_i(t)| + sgn(s_i(t))\left(K_{sw-i}\tanh\left(s_i(t)/\rho_i\right) + \frac{\omega_0}{2H_i}{}_C D^{1-\alpha}\gamma_i(\delta,\omega)\right)\right) \tag{55}$$

By inserting $\rho_i \to 0$, we have $\tanh(s_i(t)/\rho_i) \cong sgn(s_i(t))$, which approximately leads to

$$\dot{V}(t,s(t)) \cong -\sum_{i=1}^{n}\left(\eta_i\,|s_i(t)| + \left(K_{sw-i} + sgn(s_i(t))\frac{\omega_0}{2H_i}{}_C D^{1-\alpha}\gamma_i(\delta,\omega)\right)\right) \tag{56}$$

Selecting, $K_{sw-i} \geqslant \frac{\omega_0}{2H_i}\left|{}_C D^{1-\alpha}\gamma_i(\delta,\omega)\right|$ results in

$$\dot{V}(t,s(t)) \leqslant -\sum_{i=1}^{n}\eta_i\,|s_i(t)| \leqslant -\frac{1}{n}\left(\sum_{i=1}^{n}\eta_i\right)\left(\sum_{i=1}^{n}|s_i(t)|\right) = -\Omega\,\|s_i(t)\|_1\,,\ \Omega = \frac{1}{n}\sum_{i=1}^{n}\eta_i \tag{57}$$

which implies the multi-machine power system asymptotic stability based on Theorem 1.

Moreover, for the subsystem limited to the sliding manifold $s_i(t) \to 0$ or consequently $z_{3i}(t) \to 0$, the generator dynamics (26) reduce to

$$\begin{cases}\dot{z}_{1i}(t) = -k_{1i}z_{1i}(t) + z_{2i}(t)\\ \dot{z}_{2i}(t) = -k_{2i}z_{2i}(t) + 0\end{cases} \tag{58}$$

Dynamics of (58) have the positive eigenvalues k_{1i} and k_{2i}, which guarantee its asymptotic stability ($\lim_{t\to\infty} z_{2i}(t) = 0$ and $\lim_{t\to\infty} z_{1i}(t) = 0$). □

Based on (58), high values of control gains can provide a faster convergence. On the other hand, higher control gains may magnify the control signal (46) amplitude. Therefore, k_{1i} and k_{2i} should be selected to reach a balance between convergence speed and control signal amplitude.

Remark 4

Generally, $\gamma_i(\delta,\omega)$ can be considered as a lumped disturbance, which composed of interconnection terms, model uncertainties, and disturbances.

Remark 5

Inequality (57) governed by the following Chebyshev inequality:

For $a_1 \geqslant a_2 \geqslant \cdots \geqslant a_n$ and $b_1 \geqslant b_2 \geqslant \cdots \geqslant b_n$then

$$\frac{1}{n}\sum_{i=1}^{n}a_i b_i \geqslant \left(\frac{1}{n}\sum_{i=1}^{n}a_i\right)\left(\frac{1}{n}\sum_{i=1}^{n}b_i\right) \tag{59}$$

6. SEMI-DECENTRALIZED NFSMC DESIGN

The decentralized NFSMC (47) contains the following constraints:

(1) The control law (47), usually needs the upper bound of interconnections and perturbations in order to guarantee the stability of the control systems. In general, it is not easy to obtain this knowledge in practice because of the complexity of the system. Moreover, when an unknown transient fault occurs in one subsystem, it may causes large changes in interaction bounds, which makes the calculation of the switching gain K_{sw-i} difficult. Therefore, a strategy is needed in order to approximate the unknown uncertainty, which affects the interconnected subsystems.

(2) The use of functions $sgn(s_i(t))$ and $\tanh(s_i(t)/\rho_i)$ with very small ρ_i value in (47) provokes the chattering phenomena, which can damage system and degrades $C^1[0,t]$ condition.

In this section, an adaptive fuzzy scheme is applied to approximate the interconnections and perturbations upper bound, so that the objective of stability can be achieved.

6.1. Fuzzy logic system

In this part, the fuzzy logic system is briefly discussed.

DOI: 10.1002/rnc

The basic configuration of the fuzzy system composed of a collection of fuzzy IF-THEN rules, which can be written as follows [43]:

$$Rule\ l: If\ x_1\ is\ F_1^l\ and\ \ldots\ and\ x_n\ is\ F_n^l;\ Then\ y\ is\ A^l$$

where the input vector $X = [x_1, \ldots, x_n]^T \in \mathbb{R}^n$ and the output variable $y \in \mathbb{R}$ denote the linguistic variables of the fuzzy system, $i = 1, 2, \ldots, n$ denotes the number of input for the fuzzy system and $l = 1, 2, \ldots, M$ denotes the number of the fuzzy rules, F_i^l and A^l are labels of the input and output fuzzy sets, respectively.

By using the product inference, singleton fuzzification and center average defuzzification, the fuzzy system output will be as

$$y(X) = \frac{\sum_{i=1}^{m} y^l \left(\prod_{i=1}^{n} \mu_{F_i^l(x_i)} \right)}{\sum_{i=1}^{m} \prod_{i=1}^{n} \mu_{F_i^l(x_i)}} \tag{60}$$

where $\mu_{F_i^l(x_i)}$ and $\mu_{A^l}(y^l) = 1$ are the membership function of the linguistic variables x_i and y, respectively. By introducing the concept of fuzzy basis function, (60) can be rewritten in the following form

$$y(X) = \theta^T \xi(X) \tag{61}$$

where $\theta = [y^1, \ldots, y^M]^T$ is the parameter vector and $\xi(X) = [\xi^1(X), \ldots, \xi^M(X)]^T$ is a regressive vector, which can be defined as

$$\xi^l(X) = \frac{\prod_{i=1}^{n} \mu_{F_i^l(x_i)}}{\sum_{i=1}^{m} \prod_{i=1}^{n} \mu_{F_i^l(x_i)}} \tag{62}$$

6.2. Fuzzy perturbation and interconnection approximator

Because determining the interconnections, perturbation, and also modeling uncertainties upper bound is really hard. Then, based on the universal approximation of fuzzy systems, we can rewrite the sliding surface dynamics (46) as follows:

$$\begin{aligned} {}_C D^{\alpha} s_i(t) = {} & g_i\left(z_{1i}, z_{2i}, z_{3i}\right) + \frac{\omega_0}{2H_i T'_{doi}} \Big(\Delta P_{ei}(t) + P_{mi0} - \left(x_{di} - x'_{di} \right) \\ & I_{qi}(t) I_{di}(t) + T'_{doi} Q_{ei}(t) \Delta\omega_i(t) \Big) \\ & + \lambda_i z_{3i}^{p_i/q_i}(t) - \frac{\omega_0}{2H_i T'_{doi}} k_{ci} I_{qi}(t) u_{fi}(t) + D^{-(1-\alpha)} \theta_i^T \xi_i(\Delta\omega) \end{aligned} \tag{63}$$

where $\theta_i = [\theta_{1i}, \ldots, \theta_{Mi}]^T$ is the parameter vector, $\xi_i(\Delta\omega)$ is a regressive vector, and $\Delta\omega = [\Delta\omega_1, \ldots, \Delta\omega_{j\neq i} \ldots, \Delta\omega_n]^T \in \mathbb{R}^{n-1}$ is fuzzy system input vector.

Choosing the excitation voltage as

$$\begin{aligned} u_{fi}(t) = \frac{2H_i T'_{doi}}{\omega_0 k_{ci} I_{qi}(t)} \Bigg(& g_i\left(z_{1i}, z_{2i}, z_{3i}\right) + \frac{\omega_0}{2H_i T'_{doi}} \Big(\Delta P_{ei}(t) + P_{mi0} - \left(x_{di} - x'_{di} \right) I_{qi}(t) I_{di}(t) \\ & + T'_{doi} Q_{ei}(t) \Delta\omega_i(t) \Big) + \lambda_i z_{3i}^{p_i/q_i}(t) + D^{-(1-\alpha)} \left(\eta_i s_i(t) + \hat{\theta}_i^T \xi_i(\Delta\omega) \right) \Bigg) \end{aligned} \tag{64}$$

guarantees the multi-machine power system stability with the following adaptation law

$$\dot{\hat{\theta}}_i = -\mu_i \xi_i(\Delta\omega) s_i(t) \qquad or \qquad {}_C D^{\alpha} \tilde{\theta}_i = -D^{-(1-\alpha)} \mu_i \xi_i(\Delta\omega) s_i(t) \tag{65}$$

where $\tilde{\theta}_i = \theta_i - \hat{\theta}_i$ is the parameter error vector, $\hat{\theta}_i$ is the estimation vector of the unknown parameter vector θ_i, and μ_i is a positive constant used for adaptation.

DOI: 10.1002/rnc

Proof
Using (63) and (64), the closed-loop dynamic becomes

$$\begin{aligned} {}_C D^{\alpha} s_i(t) &= D^{-(1-\alpha)} \theta_i^T \xi_i(\Delta\omega) - D^{-(1-\alpha)} \left(\eta_i s_i(t) + \hat{\theta}_i^T \xi_i(\Delta\omega) \right) \\ &= D^{-(1-\alpha)} \left(\tilde{\theta}_i^T \xi_i(\Delta\omega) - \eta_i s_i(t) \right) \end{aligned} \tag{66}$$

To study the local stability and derive the adaptation law for $\tilde{\theta}_i$, we consider the following Lyapunov function:

$$V(t, X(t)) = \alpha(\|X\|) = \|X\|_2^2 = \sum_{i=1}^{n} \|X_i\|_2^2 = \sum_{i=1}^{n} \left(\frac{1}{2} s_i^2(t) + \frac{1}{2\mu_i} \tilde{\theta}_i^T \tilde{\theta}_i \right) \tag{67}$$

where $X = [X_1, X_2, \ldots, X_n]^T$ and $X_i = \left[s_i, \ \tilde{\theta}_i^T \right]$.

Differentiating (67) along the trajectory (66) and using Property 3, one can obtain that

$$\begin{aligned} \dot{V}(t, X(t)) &= \sum_{i=1}^{n} \left(s_i(t) \dot{s}_i(t) + \frac{1}{\mu_i} \tilde{\theta}_i^T \dot{\tilde{\theta}}_i \right) \\ &= \sum_{i=1}^{n} \left(s_i(t) {}_C D^{1-\alpha} {}_C D^{\alpha} s_i(t) + \frac{1}{\mu_i} \tilde{\theta}_i^T \dot{\tilde{\theta}}_i \right) \\ &= \sum_{i=1}^{n} \left(s_i(t) \left(\tilde{\theta}_i^T \xi_i(\Delta\omega) - \eta_i s_i(t) \right) + \frac{1}{\mu_i} \tilde{\theta}_i^T \dot{\tilde{\theta}}_i \right) \\ &= \sum_{i=1}^{n} \left(-\eta_i s_i^2(t) + \tilde{\theta}_i^T \left(\xi_i(\Delta\omega) s_i(t) + \frac{1}{\mu_i} \dot{\tilde{\theta}}_i \right) \right) \end{aligned} \tag{68}$$

Inserting the adaptation law (65), leads to

$$\dot{V}(t, X(t)) \leqslant - \sum_{i=1}^{n} \eta_i s_i^2(t) \ \leqslant 0 \tag{69}$$

By using Caputo definition in (3) and Theorem 2 (Corollary), we can get

$${}_C D^{1-\alpha} V(t, X(t)) = D^{-\alpha} \dot{V}(t, X(t)) = - \sum_{i=1}^{n} \eta_i D^{-\alpha} s_i^2(t) \leqslant 0 \tag{70}$$

which guarantees the closed-loop system stability. Therefore, $s_i(t)$ and $\tilde{\theta}_i$ are bounded. Although $s_i(t)$ converges to zero, the system is not asymptotically stable, because $\tilde{\theta}_i$ is only bounded.

Note that, in addition to the interconnections, the adaptation law is capable to compensate the system modeling errors and perturbations. □

Remark 6
The adaptation law (65) is also suggested in the fractional-order form in order to have set closed-loop dynamics. It can be proofed that the fractional-order adaptation law behavior is similar to the integer-order one. To testify this idea let us take ${}_C D^{1-\alpha}$ from both sides of the fractional-order adaptation mechanism

$${}_C D^{1-\alpha} {}_C D^{\alpha} \tilde{\theta} = - {}_C D^{1-\alpha} {}_C D^{-(1-\alpha)} \mu_i \xi_i(\Delta\omega) s_i(t) \quad \rightarrow \quad \dot{\tilde{\theta}} = -\mu_i \xi_i(\Delta\omega) s_i(t) \tag{71}$$

Moreover, the stability proof of the fractional-order adaptation law is same as the integer-order one except at (68), which $\dot{\tilde{\theta}}$ should be replaced by ${}_C D^{1-\alpha} {}_C D^{\alpha} \tilde{\theta}$.

Remark 7
Although the NFSMC with fuzzy approximation can have better action against unexpected perturbations in comparison with the decentralized NFSMC, it is worthwhile to notify that the NFSMC without fuzzy approximation uses only local data, whereas adding the fuzzy approximator makes it a semi-decentralized controller [44], which means each generator needs the neighbors relative speed information. This information is reachable in a short time via Fiber-optic communication technology. Therefore, although the semi-decentralized control is a high-cost technique, but it is more accurate and reliable.

DOI: 10.1002/rnc

7. SIMULATION RESULTS

A three-generator system (where generator 3 is infinite bus) in Figure 1 is chosen to demonstrate the effectiveness of the proposed decentralized fractional-order controllers. The generator and the transmission line parameters are listed in Table II. The physical limits of excitation voltage of the machine are taken $-6 \leqslant E_{fi} = u_{fi} \leqslant 6$.

The performance of the proposed controller is demonstrated in the following operating point:

$$\begin{array}{lll} \delta_{10} = 0.532\,rad, & P_{m10} = 0.57\,p.u., & V_{t10} = 1.12\,p.u. \\ \delta_{20} = 0.567\,rad, & P_{m20} = 0.56\,p.u., & V_{t20} = 1\,p.u. \end{array}$$

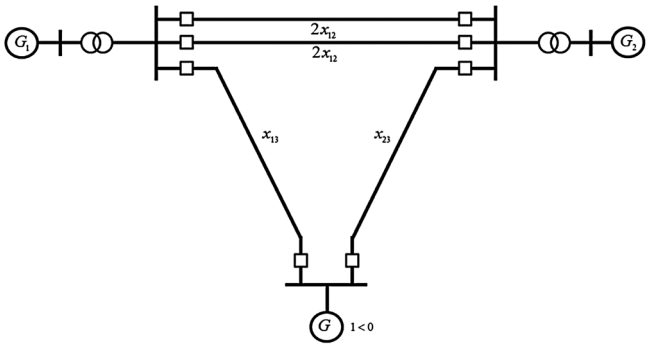

Figure 1. A two-machine infinite bus power system.

Table II. The two-machine infinite bus power system parameters.

Parameters	Generator #1	Generator #2	
$x_d(p.u.)$	1.863	2.36	
$x_d^{'}(p.u.)$	0.257	0.319	
$x_T(p.u.)$	0.129	0.11	
$x_{ad}(p.u.)$	1.712	1.712	$x_{12} = 0.15\,p.u.$
$T_{do}^{'}(sec)$	6.9	7.96	$x_{13} = 0.53\,p.u.$
$H(sec)$	4	5.1	$x_{23} = 0.6\,p.u.$
$D(p.u.)$	5	3	
k_c	1	1	$T_{do}^{'} = T_{do-min}^{'} = T_{do-max}^{'}$
$E_f(p.u.)$	[-6,6]		
$\omega_0(rad/sec)$	314.159		

$$\mu_{PBi}(\Delta\omega_j) = \frac{1}{\left(1 + \exp\left(-5 \times (\Delta\omega_j - 2)\right)\right)}$$

$$\mu_{PSi}(\Delta\omega_j) = \exp\left(-(\Delta\omega_j - 1)^2\right)$$

$$\mu_{Zi}(\Delta\omega_j) = \exp(-(\Delta\omega_j)^2)$$

$$\mu_{NSi}(\Delta\omega_j) = \exp\left(-(\Delta\omega_j + 1)^2\right)$$

$$\mu_{PBi}(\Delta\omega_j) = \frac{1}{\left(1 + \exp\left(5 \times (\Delta\omega_j + 2)\right)\right)}$$

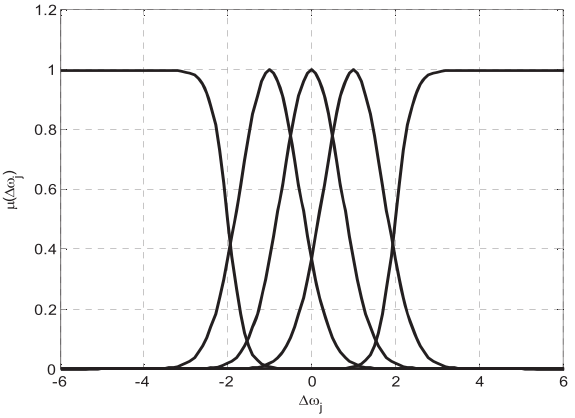

Figure 2. Fuzzy sets assigned to input variables.(generator #1: $\Delta\omega_2$ and $\Delta\omega_3$ generator #2: $\Delta\omega_1$ and $\Delta\omega_3$).

DOI: 10.1002/rnc

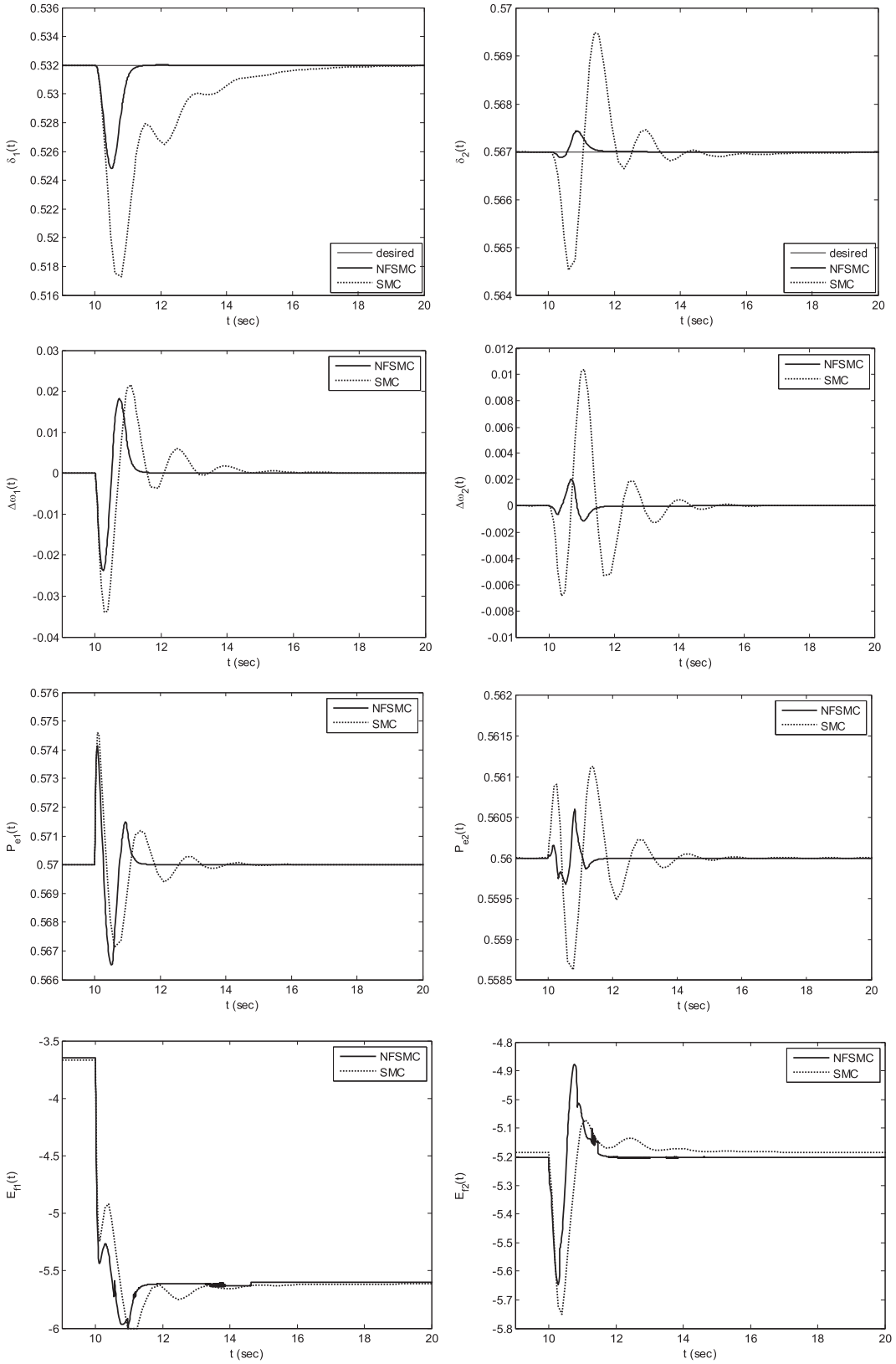

Figure 3. Power angle, relative speed, active power and excitation voltages of generators #1 and #2 for Fault 1 (NFSMC vs. SMC) with fuzzy approximator.

DOI: 10.1002/rnc

To assess the dynamic performance of the proposed controllers, we consider the following two faults in which there exists the unknown perturbation in the mechanical power P_{m0}, reactance x_d and transient reactance $x_d^{'}$:

Fault 1: Unknown perturbation transpires in the direct axis reactance and the direct axis transient reactance of generator #1 when the whole system is operating at the steady-state, and the reactance and transient reactance never recovered, that is,

$$x_{d1} = \begin{cases} 1.863 & 0 \leqslant t < 10 \\ 2.608 & 10 \leqslant t \end{cases}, \qquad x_{d1}^{'} = \begin{cases} 0.257 & 0 \leqslant t < 10 \\ 0.360 & 10 \leqslant t \end{cases}$$

Fault 2: Unknown perturbation occurs to the mechanical power of generator #1 when the whole system is operating at steady-state, and after 1 sec the mechanical power is recovered, that is,

$$P_{m10} = \begin{cases} 0.57 & 0 \leqslant t < 10 \\ 0.46 & 10 \leqslant t < 11 \\ 0.57 & 11 \leqslant t \end{cases}$$

7.1. Semi-decentralized NFSMC

Relative speed of neighbor generators are chosen as the fuzzy system input variables. Five fuzzy sets for each input variable have been found sufficient. Fuzzy sets for inputs are defined according to the membership functions depicted in Figure 2.

The controller parameters are selected as

$$\alpha = 0.2 \quad \lambda_1 = \lambda_2 = 1 \quad p_1/q_1 = p_2/q_2 = 3/11 \quad \eta_1 = \eta_2 = 10 \quad \mu_1 = \mu_2 = 40$$

also, the NBC technique control gains are considered as $k_{11} = k_{12} = 4$ and $k_{21} = k_{22} = 8$.

The simulation results of NFSMC and SMC are given in Figures 3 and 4. Both methods use the same fuzzy approximator, and SMC parameter $\eta_{1,2}$ is considered 10 to have a fair comparison. Figure 3, presents power angle, relative speed, active power and excitation voltages of generators

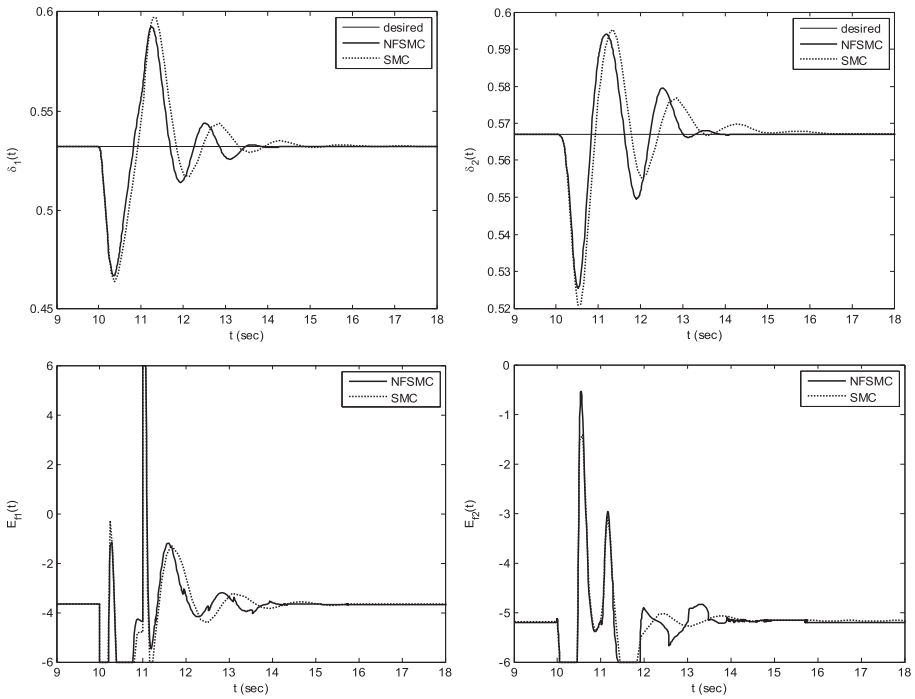

Figure 4. Power angle and excitation voltages of generators #1 and #2 for Fault 2 (NFSMC vs. SMC) with fuzzy approximator.

DOI: 10.1002/rnc

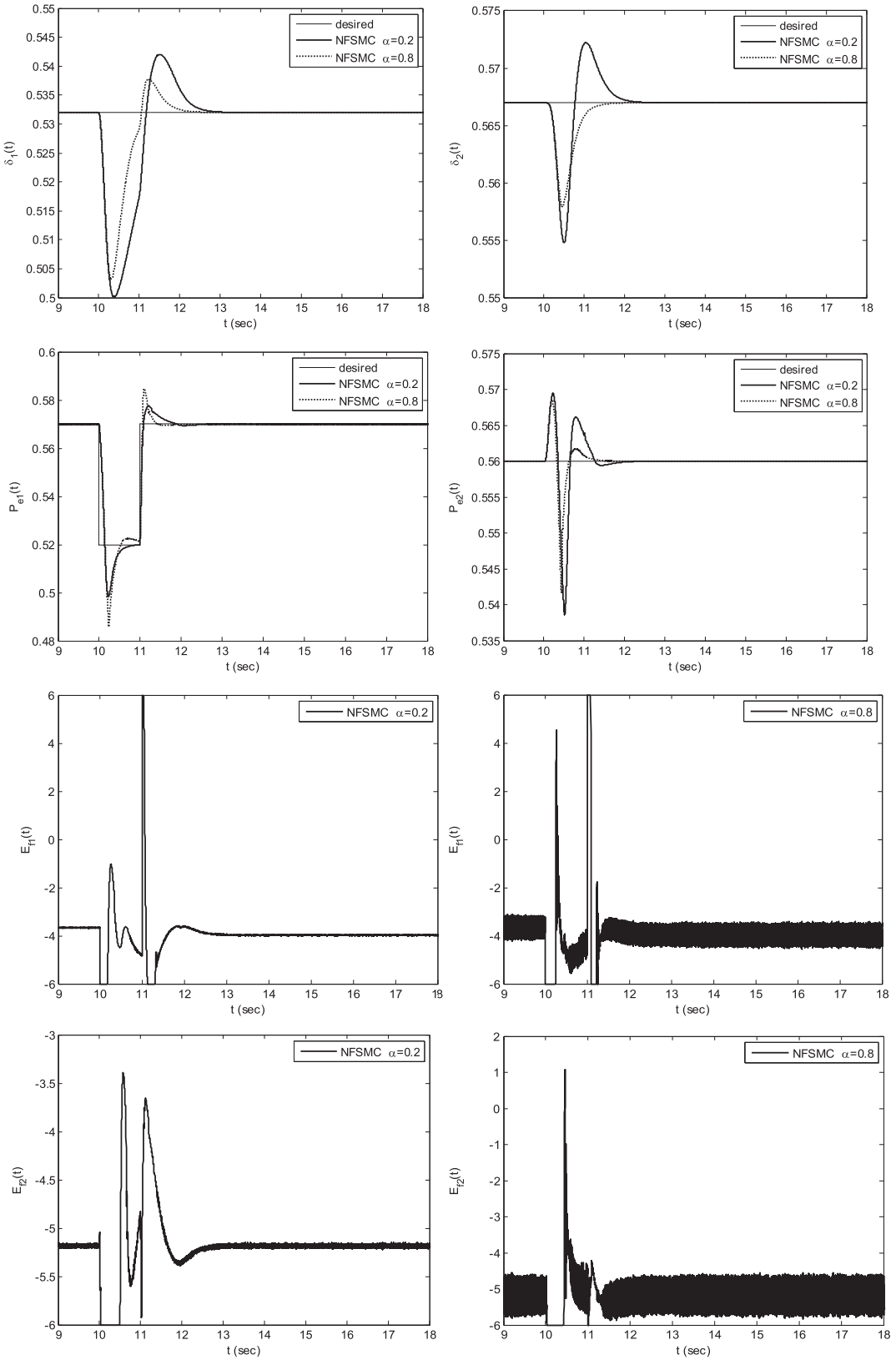

Figure 5. Power angle, active power and excitation voltages for $\alpha = 0.2 \, and \, 0.8$ of NFSMC without fuzzy approximator for half value of Fault 2.

DOI: 10.1002/rnc

Table III. Decentralized nonlinear fractional-order sliding mode controllers comparison results for $\alpha = 0.2$ *and* 0.8.

	Deviation from set point (overshoot & undershoot)		Transient response convergence time (after $t = 11$)	Control signal oscillations for $\tanh(s_i(t)/\rho_i)$
	$P_{e1}(t)$	$\delta_1(t)$, $\delta_2(t)$, $P_{e2}(t)$		
For small values of fractional parameter ($\alpha = 0.2$)	Deviation is low due to the $D^{-0.2}z_{3i}^{p_i/q_i}(t)$ integral term in the sliding surface	Deviation is high	$\delta_1(t) \cong 1.8$ sec $\delta_2(t) \cong 1.8$ sec $P_{e1}(t) \cong 1.4$ sec $P_{e2}(t) \cong 1.8$ sec	$E_{f1,2}$ chattering is low because of 0.8 -order integration $D^{-(1-\alpha)}\tanh(s_i(t)/\rho_i)$ $= D^{-0.8}\tanh(s_i(t)/\rho_i)$
For big values of fractional parameter ($\alpha = 0.8$)	Deviation is high due to the $D^{-0.8}z_{3i}^{p_i/q_i}(t)$ integral term in the sliding surface	Deviation is low	$\delta_1(t) \cong 1.4$ sec $\delta_2(t) \cong 1$ sec $P_{e1}(t) \cong 1$ sec $P_{e2}(t) \cong 0.8$ sec	$E_{f1,2}$ chattering is high because of 0.2 -order integration $D^{-(1-\alpha)}\tanh(s_i(t)/\rho_i)$ $= D^{-0.2}\tanh(s_i(t)/\rho_i)$

DOI: 10.1002/rnc

#1 and #2 for Fault 1. Also, power angle and excitation voltages of generators #1 and #2 for Fault 2 are illustrated in Figure 4. The response of NFSMC appears to be very satisfactory because it has at least 4 to 6 s faster convergence, low tracking error and generally low deviation from the operation point in comparison with the SMC.

7.2. *Decentralized NFSMC and alpha Effects*

In this part, the fuzzy term is removed and $\eta_{1,2}$ assumed to be zero in order to clarify the pure effects of the parameter α on the closed-loop system. Consider the control law (47) with the following parameters:

$$\lambda_1 = \lambda_2 = 1 \quad p_1/q_1 = p_2/q_2 = 3/11 \quad K_{sw-1} = K_{sw-2} = 50 \quad \rho_1 = \rho_2 = 0.001$$

Figure 5 shows power angle, active power, and excitation voltage signals for two different fractional parameter values ($\alpha = 0.2$ and 0.8), and exact comparison results are listed in Table III. In this table, better characteristics are highlighted with gray color. These results are governed for half value of Fault 2, which is transpired in generator #1. In this part, the Fault value is selected small in order to avoid losing the system dominant behaviors due to the control signal saturation.

In Table III, three quantities (Overshoot and Undershoot, Convergence speed, and control signal oscillations) have been presented:

(1) Overshoot and Undershoot: Higher values of α increase the integration $D^{-\alpha} z_{3i}^{p_i/q_i}(t)$ effects on the sliding surface and multiply the active power deviation from set point for $P_{e1}(t)$. Therefore, based on (58), the first generator power angle $\delta_1(t)$ overshoot decreases. These changes affect the second generator $\delta_2(t)$ and $P_{e2}(t)$ through interconnections.

(2) Convergence speed: by a glance on Figure 5 and Table III, it can be seen that the transient response convergence speed is small and better for $\alpha = 0.8$.

(3) Control signal oscillations: the excitation voltage oscillations are decreased for $\alpha = 0.2$ because of amplifying the integration effect of $\tanh(s_i(t)/\rho_i)$, which makes it a smoother function.

It is worthwhile to notify that ρ_i and p_i/q_i have direct effects on control signal chattering, tracking error and convergence time. Table IV is useful in choosing proper values for ρ_i and p_i/q_i to obtain a balance results.

7.3. *Terminal Voltage Regulation*

All previous discussions were about developing new types of PSSs without considering post-fault terminal voltage deviations. Nevertheless, because the terminal voltage V_{ti} is a function of load

Table IV. ρ_i and p_i/q_i variation effects on system behavior.

	$p_i/q_i \to 0$	$p_i/q_i \to 1$		$\rho_i \to 0$	$\rho_i \to 1$ *and bigger*
Chattering	Increase	Decrease	Chattering	Increase	Decrease
Convergence speed	Increase	Decrease	Tracking error	Decrease	Increase

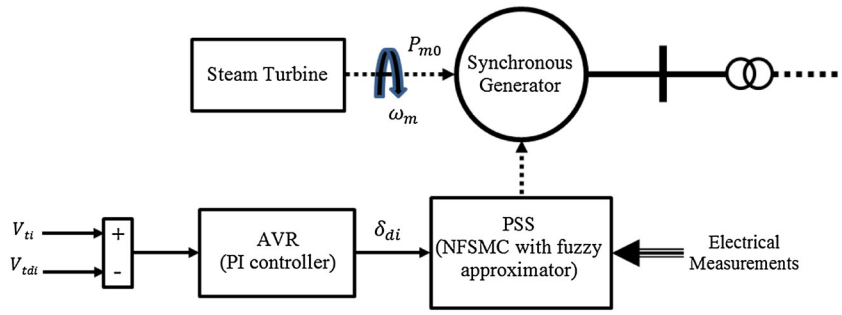

Figure 6. i-th generator control system configuration.

DOI: 10.1002/rnc

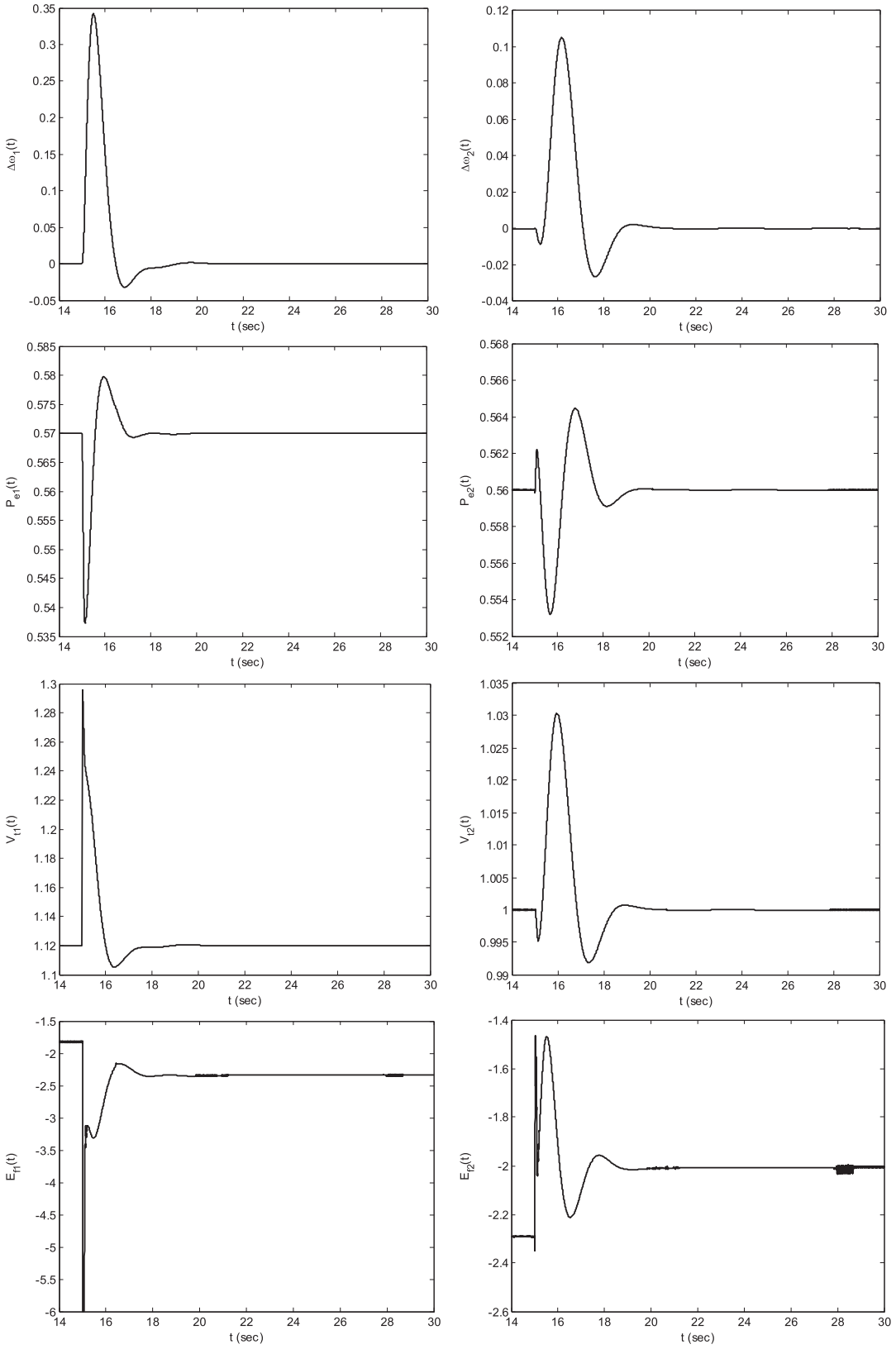

Figure 7. Relative speed, active power, terminal voltage and excitation voltages of generators #1 and #2 for Fault 1.

DOI: 10.1002/rnc

angle δ_i, active power P_{ei} and system structure, any change in the system will cause the terminal voltage to reach another equilibrium point [45]. In order to deal with this problem, we combined the NFSMC (with the fuzzy approximator) power system stabilizer with a proportional-integral (PI) regulator which generates the load angle reference value [46].

$$\delta_{di}(t) = K_{Pi}(V_{ti} - V_{tdi}) + K_{Ii}\int (V_{ti} - V_{tdi})dt \tag{72}$$

where K_{Pi} and K_{Ii} are PI parameters and must be tuned for moving δ_{di} slowly.

A simplified configuration of the aforementioned technique is presented in Figure 6, which is composed of suggested fractional PSS and a PI-based automatic voltage regulator. The performance and effectiveness of mentioned technique is illustrated in Figure 7. This figure shows relative speed, active power, terminal voltage, and excitation voltages of generators #1 and #2 for Fault 1. From Figure 7, it is evident that the rotor speed oscillations are damped down for both generators in a short time. Moreover, the terminal voltages are recovered to desired values for the proposed strategy.

8. CONCLUSION

In this paper, the idea of transient stability enhancement via NFSMC with fuzzy approximator has been employed to the multi-machine power system, and results are compared with the conventional SMC. For NFSMC with fuzzy term, the simulation results demonstrate a fast, high precision and low deviation transient response versus SMC. Moreover, the fractional parameter α absolute effects on the closed-loop system transient response and control signal chattering have been studied. When α is approaching one, it will cause a fast transient response, high excitation voltage chattering, and the electrical power high deviation (against power angle deviation). Besides when α is selected near zero, it will cause a slow transient response, low excitation voltage chattering and the electrical power low deviation. Consequently, we have an extra tuning parameter to reach a trade-off among the power angle deviation, convergence speed, and excitation voltage chattering. Finally, the suggested NFSMC PSS is combined with a simple automatic voltage regulator in order to keep the system synchronism and halter the terminal voltage variations at the same time. Simulation results reveal the effectiveness of the proposed strategy.

For future works, we intended to develop fractional-order voltage regulators and various combinations of them with the fractional-order PSSs.

REFERENCES

1. Kundur P. *Power System Stability and Control*. McGraw Hill: New York, 1994.
2. Machowski J, Bialek JW, Bumby JR. *Power System Dynamics and Stability*. John Wiley & Sons: Chichester, UK, 1997.
3. Wang Y, Guo Y, Hill D J. Robust decentralized nonlinear controller multimachine power systems. *Automatica* 1997; **33**:1725–1733.
4. Guo Y, Hill DJ, Wang Y. Nonlinear decentralized control of large-scale power systems. *Automatica* 2000; **36**: 1275–1289.
5. Jung K, Kim KY, Yoon TW, Jang G. Decentralized control for multimachine power systems with nonlinear interconnections and disturbances. *International Journal of Control, Automation, and Systems* 2005; **3**(2):270–277.
6. Yan R, Dong ZY, Saha TK, Majumder R. A power system nonlinear adaptive decentralized controller design. *Automatica* 2010; **46**:330–336.
7. Young KD, Utkin VI, Uzguner U. A control engineer's guide to sliding mode control. *IEEE Transactions on Control System Technology* 1999; **7**(3):328–342.
8. Loukianov AG, Cañedo JM, Utkin VI, Cabrera-Vázquez J. Discontinuous controller for power systems: sliding-mode block control approach. *IEEE Transactions on Industrial Electronics* 2004; **51**(2):340–353.
9. Cabrera-Vázquez J, Loukianov AG, Cañedo JM, Utkin VI. Robust controller for synchronous generator with local load via VSC. *Electric Power Energy Systems* 2007; **29**:348–359.
10. Huerta H, Loukianov AG, Cañedo JM. Multimachine power-system control:integral-SM approach. *IEEE Transactions on Industrial Electronics* 2009; **56**(6):348–359.
11. Huerta H, Loukianov AG, Cañedo JM. Decentralized sliding mode block control of multimachine power systems. *Electric Power Energy Systems* 2010; **32**:1–11.
12. Yan XG, Edwards C, Spurgeon SK, Bleijs JAM. Decentralised sliding-mode control for multimachine power systems using only output information. *IEE Proceedings-Control Theory and Applications* 2004; **151**(5):627–635.

DOI: 10.1002/rnc

13. Vega AC, Leon-Morales J, Fridman L, Pena OS, Mata-Jimenez MT. Robust excitation control design using sliding-mode technique for multimachine power systems. *Electric Power Systems Research* 2008; **78**:1627–1634.
14. Benahdouga S, Boukhetala D, Boudjema F. Decentralized high order sliding mode control of multimachine power systems. *Electric Power Energy Systems* 2012; **43**:1081–1086.
15. Chung CW, Chang Y. Design of a sliding mode controller for decentralised multi-input systems. *IET Control Theory and Applications* 2011; **5**:221–230.
16. Vargas JF, Ledwich G. Variable structure control for power systems stabilization. *Electric Power Energy Systems* 2010; **32**:101–107.
17. Podlubny I. *Fractional Differential Equations*. Academic Press: New York, 1999.
18. Luo Y, Chen YQ, Pi Y. Experimental study of fractional order proportional derivative controller synthesis for fractional order systems. *Mechatronics* 2011; **21**:204–214.
19. Cao J, Ma C, Jiang Z, Liu S. Nonlinear dynamic analysis of fractional order rub-impact rotor system. *Communications in Nonlinear Science and Numerical Simulation* 2011; **16**:1443–1463.
20. Laskin N. Fractional market dynamics. *Physica A* 2000; **287**:482–492.
21. Petras I, Magin RL. Simulation of drug uptake in a two compartmental fractional model for a biological system. *Communications in Nonlinear Science and Numerical Simulation* 2011; **16**:4588–4595.
22. Ezzat M A. Theory of fractional order in generalized thermoelectric MHD. *Applied Mathematical Modelling* 2011; **35**:4965–4978.
23. Gafiychuk V, Datsko B, Meleshko V. Mathematical modeling of time fractional reaction–diffusion systems. *Journal of Computational and Applied Mathematics* 2008; **220**:215–25.
24. Tavazoei MS, Haeri M. Synchronization of chaotic fractional-order systems via active sliding mode controller. *Physica A* 2008; **387**:57–70.
25. Hosseinnia SH, Ghaderi R, Ranjbar A, Mahmoudian M, Momani S. Sliding mode synchronization of an uncertain fractional order chaotic system. *Computers and Mathematics with Applications* 2010; **59**:1637–1643.
26. Aghababa MP. Finite-time chaos control and synchronization of fractional-order nonautonomous chaotic (hyper-chaotic) systems using fractional nonsingular terminal sliding mode technique. *Nonlinear Dynamics* 2012; **69**: 247–261.
27. Yin C, Dadras S, Zhong SM, Chen YQ. Control of a novel class of fractional-order chaotic systems via adaptive sliding mode control approach. *Applied Mathematical Modelling* 2013; **37**:2469–2483.
28. Aghababa MP. A novel terminal sliding mode controller for a class of non-autonomous fractional-order systems. *Nonlinear Dynamics* 2013; **73**:679–688.
29. Chen YQ. Ubiquitous fractional order controls? *Proceedings of the Second IFAC Workshop on Fractional Differentiation and its Applications*, Porto (ISEP), Portugal, 2006; 481–492.
30. Efe MÖ. Fractional fuzzy adaptive sliding-mode control of a 2-DOF direct-drive robot arm. *IEEE Transactions on Systems, Man, and Cybernetics—Part B* 2008; **38**:1561–1570.
31. Melicio R, Mendes VMF, Catalao JPS. Fractional-order control and simulation of wind energy systems with PMSG/full-power converter topology. *Energy Conversion and Management* 2010; **51**:1250–1258.
32. Zhang BT, Pi YG, Luo Y. Fractional order sliding-mode control based on parameters auto-tuning for velocity control of permanent magnet synchronous motor. *ISA Transactions* 2012; **51**:649–656.
33. Tang Y, Zhang X, Zhang D, Zhao G, Guan X. Fractional-order sliding mode controller design for antilock braking systems. *Neurocomputing* 2012; **111**:122–130.
34. Chang YH, Wu C, Chen HC, Chang CW, Lin HW. Fractional-Order Integral Sliding-Mode Flux Observer for Sensorless Vector-Controlled Induction Motors. *American Control Conference*, San Francisco, USA, 2011; 190–195.
35. Dadras S, Momeni HR. Fractional terminal sliding mode control design for a class of dynamical systems with uncertainty. *Communications in Nonlinear Science and Numerical Simulation* 2012; **17**:367–377.
36. Loukianov AG. Robust block decomposition sliding mode control design. *Mathematical Problems In Engineering* 2002; **8**:349–365.
37. Loukianov AG, Toledo BC, Dodds S. Robust stabilization of a class of uncertain system via block decomposition and VSC. *International Journal of Robust and Nonlinear Control* 2002; **12**:1317–1338.
38. Hewitt E, Stromberg K. *Real and Abstract Analysis*. Springer-Verlag: Berlin, 1965.
39. Li C, Deng W. Remarks on fractional derivatives. *Applied Mathematics and Computation* 2007; **187**:777–784.
40. Li Y, Chen YQ, Podlubny I. Stability of fractional-order nonlinear dynamic systems: lyapunov direct method and generalized Mittag_Leffler stability. *Computers and Mathematics with Applications* 2010; **59**:1810–1821.
41. Li Y, Chen YQ, Podlubny I. Mittag_Leffler stability of fractional order nonlinear dynamic systems. *Automatica* 2009; **45**:1965–1969.
42. Zhang F, Li C, Chen YQ. Asymptotical stability of nonlinear fractional differential system with caputo derivative. *International Journal of Differential Equations* 2011; **2011**:1–12. Article ID 635165.
43. Wang LX. *A Course in Fuzzy System and Control*. Prentice-Hall: Upper Saddle River, 1997.
44. Yousef H, Hamdy M, Madbouly E. Robust adaptive fuzzy semi-decentralized control for a class of large-scale nonlinear systems using input–output linearization concept. *International Journal of Robust and Nonlinear Control* 2010; **20**:27–40.
45. Guo Y, Hill DJ, Wang Y. Global transient stability and voltage regulation for power systems. *IEEE Transactions on Power Syatems* 2001; **16**(4):678–688.
46. Leon AE, Solsona JA, Valla MI. Comparison among nonlinear excitation control strategies used for damping power system oscillations. *Energy Conversion and Management* 2012; **53**:55–67.

DOI: 10.1002/rnc